JKAU: Eng. Sci., **vol. 12 no. 2,** pp. 83-99 (1420 A.H. / 2000 A.D.)

Laminar Natural Convection in a Square Enclosure with Discrete Heating of Vertical Walls

ABDULHAIY M. RADHWAN and GALAL M. ZAKI
Mechanical Eng. Dept., King Abdulaziz University
Jeddah , Saudi Arabia

ABSTRACT. Natural convection heat transfer in a square air-filled enclosure with one discrete flush heater is examined numerically. The enclosure is vertical with isothermal heating strip on one wall, the remainder of the wall and the opposing one are isothermally maintained at a lower temperature. The top and bottom sides are adiabatic. The two dimensional differential conservation equations of mass, momentum and energy are solved by a finite difference method for Rayleigh number varying from 10^2 to 10^6. The changes in temperature and flow fields (stream functions) with increase in Rayleigh number are investigated for different heater locations. The isothermal cold sections adjacent to the heater assist the development of secondary circulation cells, that depend upon both Rayleigh number and the position. With discrete heating and cooling sections on one wall, the flow is characterized by boundary layers lining these sections with separate circulation cells. The variation of the local Nusselt number is influenced by this flow pattern and the average Nusselt number is higher than that of a discrete heating strip mounted on an adiabatic wall. The optimum location over the range of Rayleigh number is for the heater mounted at the center of the wall, $s/L = 0.5$ a result confirmed by previous experiments.

1. Introduction

Heat transfer by buoyancy driven flow is of importance for a large number of engineering applications. Cooling of electronic equipment[1], ventilation of buildings[2], thermal performance of heat storage tanks, solar ponds and solar collectors[3,4,5] are some of the applications. The importance of free convection heat transfer phenomena taking place in enclosures is recognized by the abundant research works reviewed by Ostrach[6] and Yang[7].

Two dimensional natural convection in a differentially heated square enclosure has been solved numerically, de Vahl Davis[8], Markatos[9] and Barakos[10], Solutions agree well for the region of laminar flow, Ra $\leq 10^6$. Cochran[11] presented comparison of the computational methods extending the enclosure problem to account for temperature dependent viscosity. Various configurations for enclosures have been investigated using different solution techniques and for different side heating conditions, such as asymmetrically heated opposite vertical[12-14] or inclined[15,16] sides and discrete wall heating[17-23]. The scope of these studies covered a wide range of parameters influencing the heat transfer process such as the number of discrete heaters[17, 18], the cavity width[19], effect of Prandtl number[20], effect of aspect ratio[21] and the discrete heat source location[22].

The work of Chu and Churchill[23] is a major contribution to the problem of discrete heating in vertical enclosures, where a finite difference solution is presented for a wide range of parameters (aspect ratio (.4-5) and Grashof number from 10^2 to 10^5). The effect of the size and location of the strip heater upon Nusselt number was also investigated. The maximum average Nusselt number depends upon Groshof number and the distance between the strip heater and the top of the enclosure. Hadim[24] considered two discrete heaters flush mounted on the two opposite vertical sides of a square cavity.

This study is a contribution to the ongoing research effort for enhancing the convection heat transfer in enclosures. It is suggested here to introduce successive discrete heating and cooling strips on the same vertical wall of the enclosure, this configuration has not been investigated before. The flow and temperature fields for this arrangement assist formation of eddy cells that influence the overall convection rate. One side is discretely heated with a flush heating strip at constant high temperature and the rest of this side as well as the opposite side are isothermal heat sinks. The top and bottom sides are insulated and the enclosure is filled with a Newtonian temperature dependent density fluid.

2. Mathematical Formulation and Numerical Computation

The configuration of interest for the present study is shown in Fig. 1, which is two dimensional square enclosure with a side of length L and adiabatic top and bottom walls. The left vertical side has a flush discrete heater at a constant temperature, T_h. The rest, ℓ_1 y > ℓ_2, of the wall as well as the right side, $X = 1$, are kept at a lower temperature T_c. The hot isothermal strip is located between $y = \ell_1$ and $y = \ell_2$, Fig. 1, and the fluid inside the enclosure is assumed incompressible, Newtonian with density variation only pertinent to temperature changes. The governing mass, momentum (x and y directions) and energy conservation equations for steady state buoyancy driven fluid flow are:

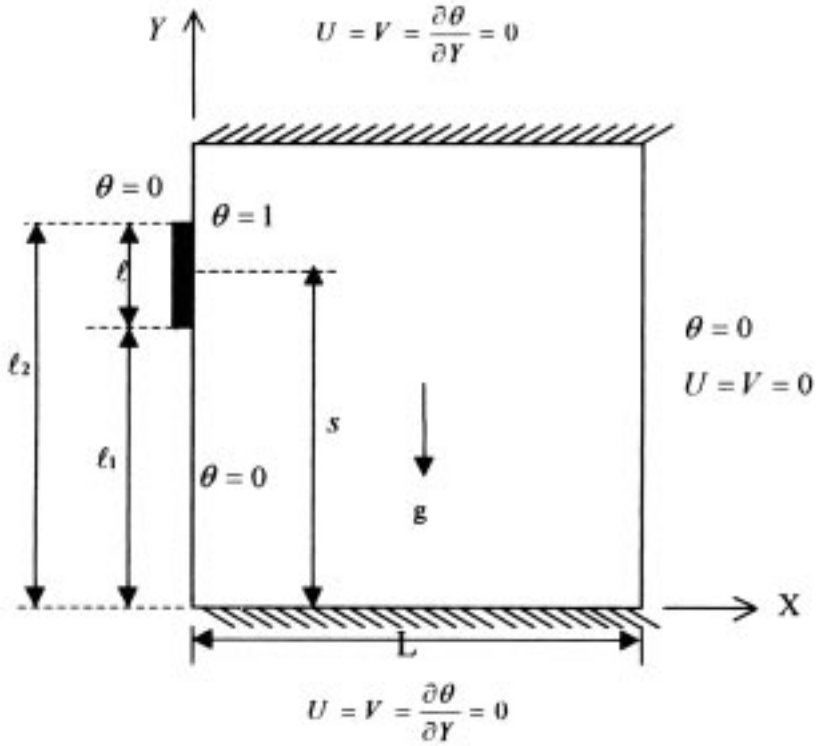

FIG. 1. Schematic of enclosure configurations.

$$\frac{\partial u}{\partial x} + \frac{\partial v}{\partial y} = 0 \tag{1}$$

$$\rho_c \left(u \frac{\partial u}{\partial x} + v \frac{\partial u}{\partial y} \right) = -\frac{\partial P}{\partial x} + \mu \left[\frac{\partial^2 u}{\partial x^2} + \frac{\partial^2 u}{\partial y^2} \right] \tag{2}$$

$$\rho_c \left(u \frac{\partial v}{\partial x} + v \frac{\partial v}{\partial y} \right) = -\frac{\partial P}{\partial y} - \rho g + \mu \left[\frac{\partial^2 v}{\partial x^2} + \frac{\partial^2 v}{\partial y^2} \right] \tag{3}$$

$$u \frac{\partial T}{\partial x} + v \frac{\partial T}{\partial y} = \frac{k}{\rho_c c_p} \left(\frac{\partial^2 T}{\partial x^2} + \frac{\partial^2 T}{\partial y^2} \right) \tag{4}$$

Eliminating the pressure gradient terms in Eqs. 2 and 3 by cross partial differentiation and introducing the vorticity function:

$$\omega = \frac{\partial V}{\partial X} - \frac{\partial U}{\partial Y} \tag{5}$$

into Equation (1) making use of the following dimensionless variables:

$$U = \frac{uL}{\upsilon} = \frac{\partial \psi}{\partial Y} \quad , \quad Y = \frac{y}{L}$$

$$V = \frac{vL}{\upsilon} = -\frac{\partial \psi}{\partial X} \quad , \quad X = \frac{x}{L}$$

$$\theta = \frac{T - T_c}{T_h - T_c} \quad , \quad \mathrm{Gr} = \frac{g\beta L^3 (T_h - T_c)}{\upsilon^2}$$

Equations (1) through (4) are written in the following dimensionless form (known as steady-state derived variables convection equations):

$$\frac{\partial^2 \psi}{\partial X^2} + \frac{\partial^2 \psi}{\partial Y^2} = \; . \; \omega \tag{6}$$

$$U\frac{\partial \omega}{\partial X} + V\frac{\partial \omega}{\partial Y} = \left[\frac{\partial^2 \omega}{\partial X^2} + \frac{\partial^2 \omega}{\partial Y^2}\right] + Gr\frac{\partial \theta}{\partial X} \tag{7}$$

$$U\frac{\partial \theta}{\partial X} + V\frac{\partial \theta}{\partial Y} = \frac{1}{\mathrm{Pr}}\left[\frac{\partial^2 \theta}{\partial X^2} + \frac{\partial^2 \theta}{\partial Y^2}\right] \tag{8}$$

where ψ is the normalized stream function. For free convection, the governing dimensionless parameters are Grashof and Prandtl numbers.

The boundary conditions of velocity and temperature fields are shown in Fig. 1 and presented as:

$$X = 0 : U = V = \psi = 0 \quad , \quad \begin{cases} \theta = 1 & \ell_1 / L \le Y \le \ell_2 / L \\ \theta = 0 & \text{elsewhere} \end{cases} \tag{9}$$

$$X = 1 : U = V = \psi = 0 \quad , \quad \theta = 0 \tag{10}$$

$$\left.\begin{matrix} Y = 0 \\ Y = 1 \end{matrix}\right\} : U = V = \psi = 0 \quad , \quad \frac{\partial \theta}{\partial Y} = 0 \tag{11}$$

Equation 9 is written in a general form, whereas for $\ell_1 = 0$ and $\ell_2 = 1$, the problem presents the standard enclosure conditions with one side at T_h, ($\theta = 1$), and the opposite side at T_c, ($\theta = 0$). The position of the discrete element of length ℓ is controlled by s that varies from $\ell/2$ to $(L - \ell/2)$.

The vorticity boundary condition near the wall is obtained using values of the stream function for the layers adjacent to these walls. An expression suggested by Nogotov[25] has been used for all interior surfaces of the enclosure as:

$$\omega = \frac{-8\psi_a + \psi_b}{2\delta} \quad \text{at} \quad \begin{cases} X = 0 \ , & X = 1 \\ Y = 0 \ , & Y = 1 \end{cases} \tag{12}$$

where ψ_a and ψ_b are the values of the stream function at distances δ and 2δ from the wall respectively, δ is the grid size.

The local heat transfer rate along the heated section of the wall is obtained from the heat balance that gives an expression for the local Nusselt number as:

$$\mathrm{Nu_h} = -\left.\frac{\partial\theta}{\partial X}\right|_{x=0} \quad ; \quad Y_1 \le Y \le Y_2 \tag{13}$$

where $Y_1 = \ell_1/L$ and $Y_2 = \ell_2$, Fig. 1. The average value for Nusselt number is defined by:

$$\overline{\mathrm{Nu_h}} = \frac{1}{Y_2 - Y_1} \int_{Y_1}^{Y_2} -\left.\frac{\partial\theta}{\partial X}\right|_{x=0} dY \tag{14}$$

The governing dimensionless differential equations are discretized to a finite difference form following the scheme suggested by Nogotov[25] explicit central second-order difference). The computational scheme, based on Successive Over Relaxation, SOR, is arranged to solve the three equations for the $(k + 1)$ *th* iteration step. The initial values over the field for θ, ω and ψ are assumed zero for $\mathrm{Ra} \le 10^4$, for higher values of Rayleigh number, the field values at $\mathrm{Ra} = 10^4$ are taken as initial starting values. The relaxation parameters, $\gamma_\theta = \gamma_\omega = 1$ and $\gamma_\psi = 1.6$ give stable numerical computation with 21×21 grid and $\mathrm{Ra} \le 10^4$, for higher Ra values $\gamma_\theta = 1$, $\gamma_\omega = 0.1$ to .02 and $\gamma_\psi = 1.97$ are used.

The criterion for convergence is examined according to a realistic condition for each state variable at each node as:

$$\frac{\left|\lambda_{ij}^{k+1} - \lambda_{ij}^{k}\right|}{\left|\lambda_{ij}^{k}\right|} \le \in_\lambda \tag{15}$$

where the subscripts i and j refer to a grid node, γ is a dummy space variable (θ, ω, or ψ) and $\in_\lambda$ is a small quantity set to 10^{-3} for $\mathrm{Ra} \le 10^5$ and set to 10^{-4} for $\mathrm{Ra} \ge 10^5$ in the present work for the grid of 21×21. Finer uniform grid (41×41) and $\in_\lambda = 10^{-5}$ are used to improve the results at $\mathrm{Ra} = 10^6$.

The iterative routine, the selected grid and the relaxation parameters are verified by comparing the results with corresponding previous works for a standard square enclosure ($\ell/L = 1$, s/L = 0.5, $\theta = 1$ at $X = 0$ and $\theta = 0$ at $X = 1$) at different Rayleigh numbers. The computed values of the average Nusselt numbers are in good agreement with the corresponding results of De-Vahl Davis[8], Markatos[9] and Quon[26] , for air, Pr = 0.71, as seen in Table 1.

TABLE 1. Average Nusselt number, $\bar{N}u$, in air filled square enclosure.

Ra	de-Vahl Davis [8]	Markatos [9]	Quon [26]	Present work
10^3	1.117	1.108	1.13	1.149
10^4	2.243	2.201	2.26	2.206
10^5	4.509	4.43	4.54	4.515

The solutions have also been checked for energy balance where the heat released by the hot isothermal wall equals the heat transferred to all cold walls. Discontinuity in temperature at the edges of the heater by the sudden change of temperature from $\theta = 1$ to $\theta = 0$ at $X = 0$, $y = \ell_1$ and ℓ_2 is numerically achieved by selecting small grid size (21×21) or (41×41) and impose linear temperature variation between the two adjacent nodes at the edge of the heated section, *i.e.* ($\theta = 1$ at $y = \ell_2 - \delta/2$ and $\theta = 0$ and $y = \ell_2 + \delta/2$ and a linear relation is assumed between the two locations).

3. Numerical Results

The study considers buoyancy driven motion of air (Pr = 0.71) created by a strip heater. The dimensionless length of the heater, ℓ/L, is constant at .35 *while the relative location s/L changes as 0.175, 0.5 and 0.825. These positions refer to placing the heated section at the bottom corner, the middle and at the top corner of the vertical wall respectively.

3.1 Flow and Temperature Fields

The development of the isothermal lines and stream functions as Rayleigh number varies from 10^3 to 10^6 for $s/L = 0.175$ are shown in Fig. 2. At Rayleigh number, 10^3-10^4, heat dissipated from the discrete heater develops a fluid layer

*The choice of the ratio $\ell/L = 0.35$ is mainly dictated by the condition for an ongoing experimental work, for which the heater length is 10.5 cm and the enclosure side is 30 cm. The experimental study is still in progress.

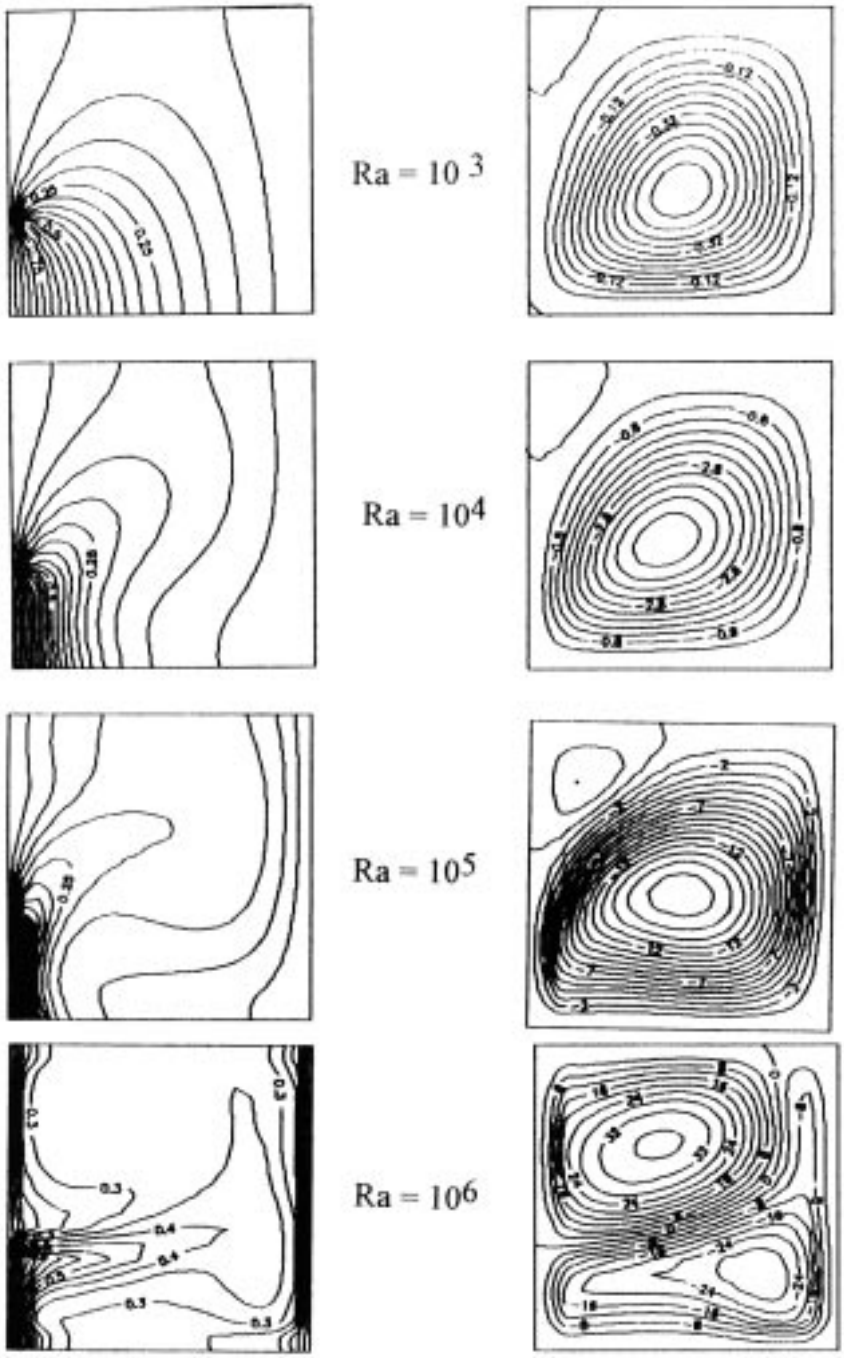

FIG. 2. Development of isotherms and stream functions with Rayleigh number for $s/L = 0.175$.

that moves upward at low velocity for Ra = 10^3 as indicated by the largely spaced isotherms to those shown for Ra = 10^4. The cold wall above the heater, suppresses this buoyancy effect. The isotherms are clustered near the hot section, in nearly parallel lines, indicating domination of diffusion heat transfer mode close to the bottom section of the heater. The hot fluid looses part of its energy to the cold section of the same wall and moves along the adiabatic ceiling then down along the right side wall forming a single central cell with a center shifted from that of the enclosure. Secondary eddy zone is formed in the upper top corner as a result of the tendency of the hot rising fluid to move away from the corner. The eddy cell size increases with increasing Rayleigh number, Fig. 2. It is noticed that the pattern of the streamlines changes with increasing Rayleigh number. The effect is pronounced at Ra = 10^6 where the main cell is distorted and prolonged to an elliptic shape in the lower part, while the upper eddy cell grows to occupy the upper portion. Steep temperature gradients are noticed along the two vertical sides and nearly vanish in the central region. The lower vortex, at Ra = 10^6, moves clockwise, and the effect of the upper vortex, rotating anticlockwise causes the distortion shown in the stream functions.

The streamlines and isotherms when the discrete heater is placed at the center of the cold vertical wall, s/L = .5 are presented in Fig. 3 for different Rayleigh numbers. The isotherms and streamlines at Ra = 10^3 show that the flow forms a single circulation cell with its center coinciding with that of the enclosure. A small eddy circulation cell appears in the upper left corner. An increase in Rayleigh number to 10^4 causes distortion of the isotherms where the heat propagates more towards the cold wall opposite to the discrete heater. The eddy cell at the top corner increases in size and a new eddy cell appears at the lower left corner.

At Ra = 10^5 the temperature gradients along the heater and the top cold section are steep, but much less at the lower cold section. This causes the upward tilt of the stream function and the elongation noticed at the center of the main circulation cell. Further increase in Rayleigh number to 10^6, Fig. 3, causes sharp temperature gradients along the vertical walls, where the boundary layers are getting thinner. The nearly horizontal isotherms in the bulk region indicate that the fluid motion occurs mainly in the boundary layers and weak vertical motion in the bulk region. The region is a multicellular now with one central and two corner cells.

When the heater is placed at the top corner, s/L = 0.825, heat is transferred from the discrete heater to both the cold opposite wall and to the section below the heater. The isothermal lines shown in Fig. 4 at Ra = 10^3 and 10^6 indicate that at low Rayleigh number one central cell is formed, and one eddy cell at the lower left corner. A situation opposite to that shown in Fig. 2 for the same Ray-

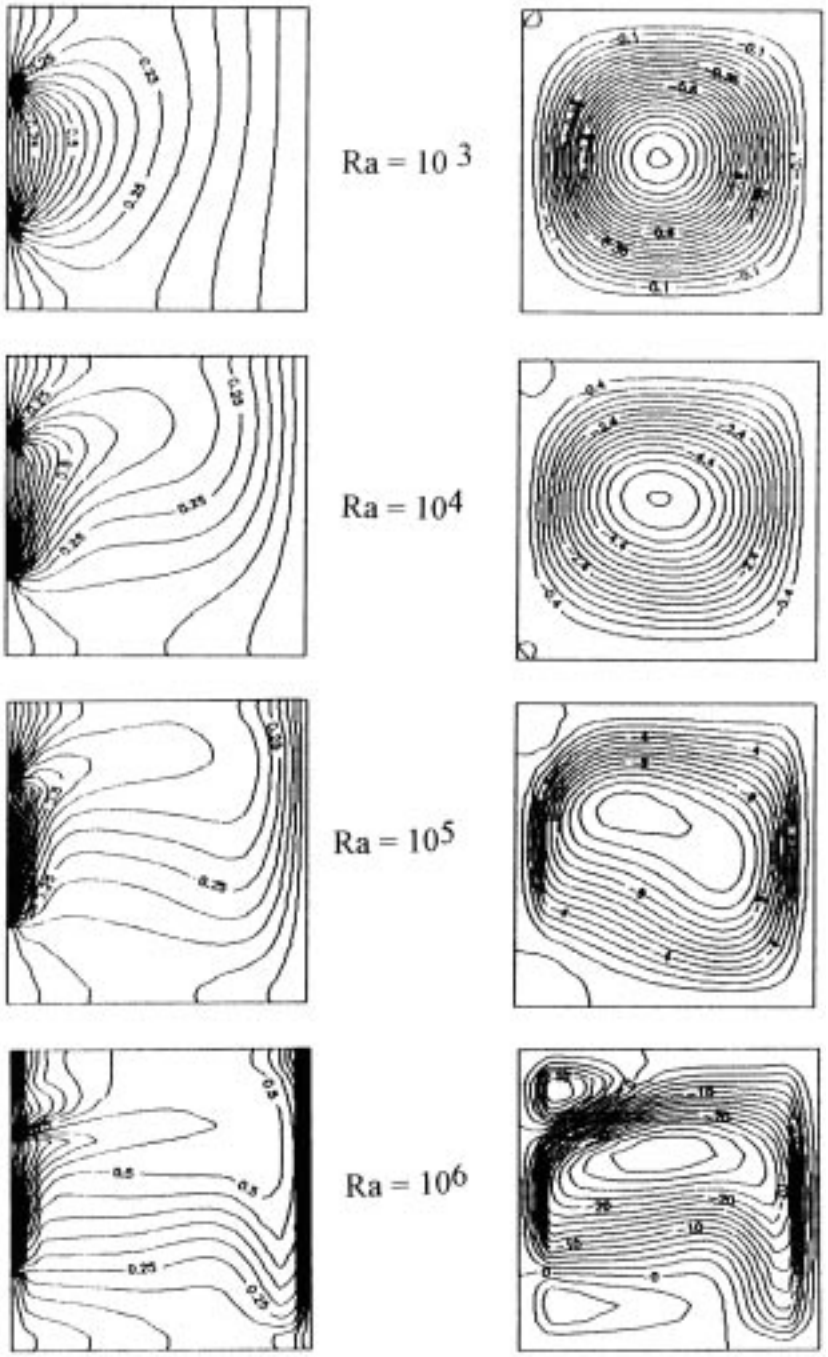

FIG. 3. Development of isotherms and stream functions with Rayleigh number for $s/L = 0.5$

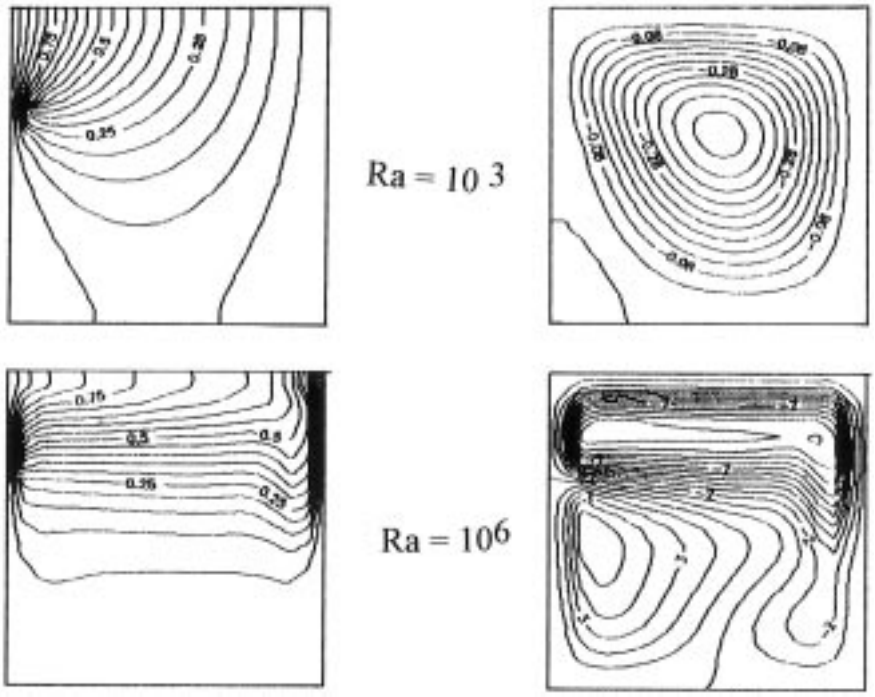

FIG. 4. Contour maps for Ra = 10^3 and 10^6 with the discrete heater location $s/L = 0.825$.

leigh number. As Rayleigh number increases from 10^3 to 10^6 the boundary layers build-up near the discrete heated section and along portion of the opposite cold wall, where convection takes place. In the central zone of the enclosure the horizontal isotherms are parallel with temperature increase in the upward direction. Though two cells are formed the lower portion of the enclosure being far from the heater is not significantly affected by the heater. The steep gradient of the isotherms near the walls indicates the extent of strength of the convective heat transport process generally measured by the magnitude of Nusselt numbers.

3.2 Nusselt Number Variation

The spatial distribution of the local Nusselt number Nu along the hot section depends on both the location s/L and Rayleigh number, Fig. 5. In the lowest position, $s/L = 0.175$, and for Ra $\leq 10^4$ diffusion is the dominating process, resulting in low Nusselt number. Nusselt number increases along the height from bottom towards the top of the hot section but at different rates, the enhancement is high near the upper edge of the hot strip.

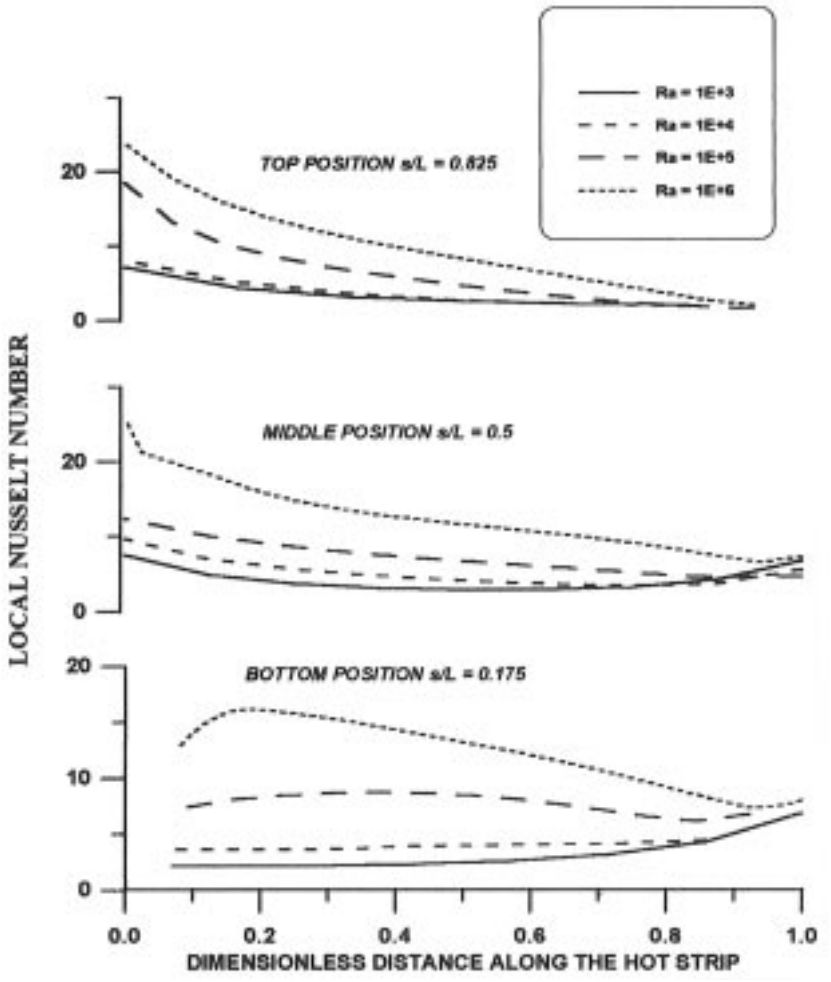

FIG. 5. Variation of local Nusselt number along the hot strip for different locations and Rayleigh numbers.

As convection is enhanced by increasing Rayleigh number to 10^5, the boundary layer becomes thinner and the velocity increases, Nusselt number reaches a maximum (Nu = 8.68) at y/ℓ =0.4 and then decreases to be 6.74 close to the edge of the heating section. The same trend is observed for Ra = 10^6, Fig. 5, but the maximum Nusselt number (Nu = 16.2) is shifted to a lower position y/ℓ = 0.15.

The spatial variation is different when the heated section is centered in the middle part of the vertical isothermal wall, s/L = 0.5. At low Rayleigh number, 10^3, the heat transfer decreases along the height of the heater reaching a mini-

mum at nearly mid plane (Nu = 2.84) and higher at the lower and upper edges (Nu = 7.8) of the heater. This trend vanishes with the increase in Rayleigh number *i.e.* enhancement of convection. The clustering of the isothermal lines adjacent to the heated section at Ra = 10^5 and 10^6, Fig. 3, suggests high temperature gradients at the lower section of the hot strip ($y/L < 0.5$) that decreases at the upper edge. This is the reason for the decrease in Nusselt number along the heater length.

The variation of Nusselt number as the discrete heater is placed at the top corner, $s/L = 0.825$ is shown also in Fig. 5. The decrease in local Nusselt number with heating strip length, Fig. 5, is experimentally confirmed by the data of Chadwick[27], for single and multiple heaters in spite of different aspect ratio.

The average Nusselt number variation for the different s/L values and Ra = 10^2-10^6 is shown in Fig. 6. The optimum location for a heater is seen to be at s/L = 0.5 for which the average Nusselt number is the highest at all values of Rayleigh number. The experimental data of Turner[28] show that for an aspect ratio of 1 the maximum $\bar{N}u$ occurs at $s/L = 0.5$ at Ra=10^5 and 0.47 at Ra = 6×10^6 which confirm the present result. Nusselt number variation for the limiting case

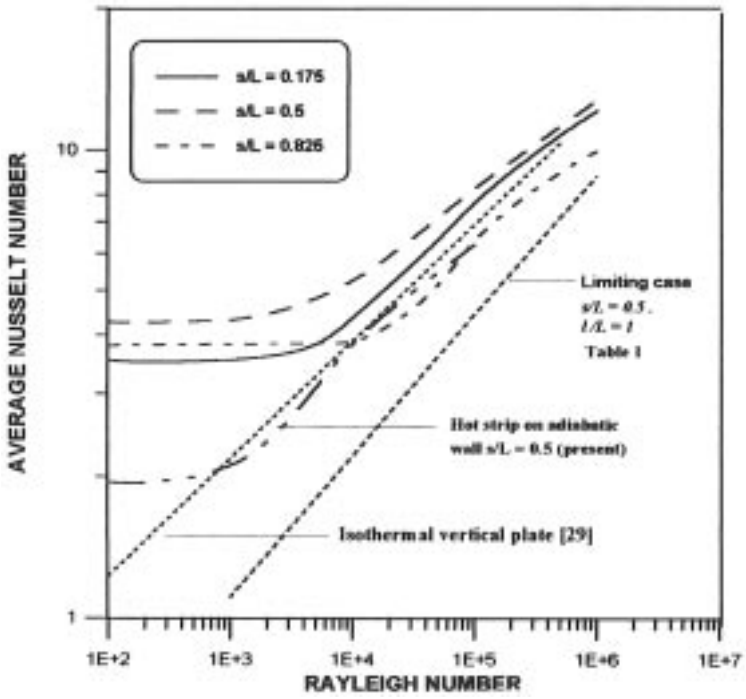

FIG. 6. Average Nusselt number dependency on Rayleigh number for different discrete heat locations.

as $s/L = 0.5$, $\ell_1 = 0$ and $\ell_2 = L$ (Table 1) is also shown in the figure, indicating that average Nusselt number for discrete heating exceeds that for a fully heated side in a square enclosure. It is of interest to note that alternate cooling and heating (the heated section is placed between two cold sinks) results in high average $\bar{N}u$. Nusselt number is constant independent of Ra between $Ra = 10^2$ up to 5×10^3 for $s/L = 0.5$ and up to 10^4 for $s/L = 0.875$ then increases with $Ra^{0.25}$, being parallel to the established relation for the isothermal plate[29]. The case for the same strip heater ($\ell/L = .35$) mounted at 0.5 is solved for $\partial\theta/\partial X = 0$ instead of $\theta = 0$ and presented in Fig. 6. It is evident that mounting a strip heater on an isothermal cold wall enhances $\bar{N}u$. significantly up to $Ra \leq 10^6$, in particular for the weak buoyancy region ($10^2 < Ra < 10^3$) $\bar{N}u. = 4.2$ versus 1.99 for adiabatic wall condition.

4. Conclusions

In this paper natural convection in an air filled square cavity with a single flush discrete heater mounted on a vertical wall is studied. The enclosure consists of top and bottom adiabatic surfaces, two isothermal vertical walls with a flush isothermal hot strip. The partial differential equations for two dimensional conservation of mass, momentum and energy are solved based on central second order finite difference method. The solution scheme is validated by comparison with well established reference solutions. The model is then used to investigate the effect of hot strip location on both heat transfer and fluid flow patterns, within the cavity for fixed heater length $\ell/L = 0.35$ and different positions, $s/L = 0.175$, 0.5 and 0.825. For the single heater, the optimal location that gives the higher heat transfer rate, average Nusselt number, is $s/L = 0.5$, compared to other locations, for all values of Rayleigh number, 10^2-10^6. The effect of the isothermal cold sections adjacent to the heater on the stream functions and isotherms is explained. This effect is more pronounced at high Rayleigh numbers where multicellular flow patterns dominate. The present data shows in general highest heat transfer rate compared with the case of adiabatic vertical wall, with one distinct heater.

Nomenclature

c_p	Specific heat at constant pressure, Ws/K kg
Gr	Grashof number
g	gravitational acceleration, m/s^2
h	heat transfer coefficient, W/m^2 K
k	thermal conductivity, W/m K
ℓ	heater length, m
ℓ_1	distance to the lower edge of the heater, m

ℓ_2 distance to the upper edge of the heater, m
L enclosure width = enclosure height, m
Nu local Nusselt number = hL/k
Nu average Nusselt number = $\overline{h}L/k$
Pr Prandtl number, $c_p\,\mu$/k
Ra Rayleigh number = Gr.Pr
T temperature, K
u,v velocity components in the x and y direction, m/s
U,V dimensionless velocity components
x,y space coordinates in cartesian system
X,Y dimensionless cartesian coordinates

Greek Symbols

β Coefficient of volumetric thermal expansion, K^{-1}
γ relaxation factor
δ dimensionless grid size
θ dimensionless temperature
μ dynamic viscosity, kg/ms
υ kinematic viscosity, m^2/s
ρ variable density = $\rho_c\,[1 - \beta\,(T - T_c)]$, kg m^{-3}
ρ_c density at T_c, Kg m^{-3}
ψ non-dimensional stream function
ω non-dimensional vorticity

Subscripts

c cold surface
h hot surface

References

[1] I**ncropera, F.P.,** Convection heat transfer in electronic equipment cooling, *ASME J. Heat Trans.* **110,** 1097-1111, (1988).

[2] **Hoogendooren, G.J.** and **Afgan, N.H.** (Eds) *Energy Conservation in Heating, Cooling and Ventilating Buildings,* Hemisphere Pub. Washington D.C. (1978).

[3] **Cha, C.K.** and **Jauria, Y.,** Recirculating Mixing Convection Flow for Energy Extraction, *Int. J. Heat Mass Transfer,* **27**, 1801-1810, (1984).

[4] **Imberger, J.** and **Hamblin, P.F.,** Dynamics of Lakes, Reservoirs and Cooling Ponds, *A. Rev. Fluid Mech.,* **14,** 153-187, (1982).

[5] **Ben Yedder, R., Du, Z.G.** and **Bilgen, E.,** Heat Transfer by Natural Convection in Composite Trombe Wall Solar Collector, *Proc. ASME, Solar Energy Technology, 1989, San Francisco* (J.T. Beard and H.C. Heuritt, editors), **8,** 7,-13 (1989).

[6] **Ostrach, S.,** Natural Convection in Enclosures, *Trans. ASME, J. Heat Transfer,* **110,** 1175-1190, (1988).

[7] **Yang, K.T.,** Natural Convection in Enclosures, In, *Handbook of Single-Phase Convective Heat Transfer,* (Edited by **S. Kakac, R. Shah** and **W. Aung**) Wiley New York, Chap. 13, (1987).

[8] **De Vahl Davis, G.,** Natural Convection of Air in a Square Cavity: A Benchmark Numerical Solution, *Int. J. Numerical Methods in Fluids,* **3,** 249-264, (1983).

[9] **Markatos, N.C.** and **Pericleous, K.A.,** Laminar and Turbulent Natural Convection in an Enclosure Cavity, *Int. J. Heat Mass Transfer,* **27,** 5, 755-772, (1984).

[10] **Barakos, G., Mitsoulis, E.** and **Assimacopoulos, D.,** Natural convection flow in a square cavity, revisited: Laminar and turbulent models with wall functions, *Int. J. for Numerical Methods in Fluids,* **18,** 695-719, (1994).

[11] **Cochran, R.J.** and **Roy, R.E.,** Comparison of Computational Results for Natural Convection in a Square Enclosure, with Variable Viscosity, Benchmark Problem, *Proc. of the 1995 ASME Cong.* Part **1,** 1112-1117, (1995).

[12] **Ozoe, H., Mouri, A., Ohmuro, M., Churchill, S.W.** and **Lior, N.,** Turbulent Convection in Water in Rectangular Channels Heated and Cooled Isothermally on the Opposing Vertical Walls, *Int. J. Heat Mass Transfer,* **28,** 1, 125-138, (1985).

[13] **Karanjiannis, T.G., Ciofala, M.** and **Barbaro, G.,** On Natural Convection in a Single and Two-Zone Rectangular Enclosures, *Int. J. Heat Mass Transfer,* **35,** 7, 1645-1657, (1992).

[14] **Wakitani, S.,** Development of Multicellular Solutions in Natural Convection in an Air-filled vertical Cavity, *ASME J. Heat Transfer,* **119,** 97, (1997).

[15] **Tzeng, P.Y., Soong, C.Y.** and **Sheu, T.S.,** Numerical Investigation of Transient Flow-Mode Transition of Laminar Natural Convection in an Inclined Enclosure, *Numerical Heat Transfer Part A: Applications* **31,** 2, 193-206, (1997).

[16] **Kuypar, R.A., Van DerMeer, Th.H.** and **Hoogendoorn, C.J.,** Numerical Sudy of Laminar and Turbulent Natural Convection in an Inclined Square Cavity, *Int. J. Heat Mass Transfer,* **36,** 3899-3911, (1993).

[17] **Keyhani, M., Prasad, V.** and **Cox, R.,** An Experimental Study of Natural Convection in a Vertical Cavity with Discrete Heat Sources, *ASME J. Heat Transfer* **110,** 616-624, (1988).

[18] **Keyhani, M., Prasad, V., Shen, R.** and **Wong, T.T.,** Free Convection Heat Transfer from Discrete Heat Sources in a Vertical Cavity. In Natural and Mixed Convection in Electronic Equipment Cooling, *ASME HTD* Vol. **100,** 13-24, (1988).

[19] **Carmona, R.** and **Keyhani, M.,** The Cavity Width Effect on Immersion Cooling of Discrete Flush-heaters on One Vertical Wall of an Enclosure Cooled from the Top, *ASME J. Electronic Packaging* **111,** 268-276, (1989).

[20] **Prasad, V., Keyhani, M.** and **Shen, R.,** Free Convection in a Discretely Heated Vertical Enclosure: Effects of Prandtl Number and Cavity Size, *ASME J. Electronic Packaging* **112,** 63-74, (1990).

[21] **Ho, C.J.** and **Chang, J.Y.,** A Study of Natural Convection Heat Transfer in a Vertical Rectangular Enclosure with Two-Dimensional Discrete Heating: Effect of Aspect Ratio, *Int. J. Heat Mass Transfer,* **37,** 6, 917-925, (1994).

[22] **Refai, G.A.** and **Yovanovich, M.M.,** Influence of Discrete Heat Source Location on Natural Convection Heat Transfer in a Vertical Square Enclosure, A*SME J. Electronic Packaging* **113,** 268-274, (1991).

[23] **Chu, H.H.** and **Churchill, S.W.,** The effect of heater size, location, aspect ratio and boundary conditions on two dimensional laminar natural convection in rectangular channels, *ASME J. Heat Transfer,* **98,** 2, 194-201, (1976).

[24] **Hadim, A.** and **Ramot, M.,** Natural Convection in an Enclosure with Discrete Heat Sources on the Vertical Walls, *Proceedings ASME Winter Conference,* 1993, Paper **93-**WA/EEP-26, (1993).

[25] **Nogotov, E.F.,** *Applications of Numerical Heat Transfer,* McGraw Hill, 100-109,(1978).

[26] **Quon, C.,** High Rayleigh Number Convection in an Enclosure: A Numerical Study, *Phys. Fluids,* Vol. **15-I,** pp. 12-19, (1972).

[27] **Chadwick, M.L., Webb, B.W.** and **Heaton, H.S.,** Natural Convection from Two-dimensional Discrete Heat Sources in a Rectangular Enclosure, *Int. J. Heat Mass Transfer,* **34,** 7, 1679-1693, (1991).

[28] **Turner, B.L.** and **Flack, R.D.,** The Experimental Measurement of Natural Convective Heat Transfer in Rectangular Enclosure with Concentrated Energy Sources, *ASME, J. Heat Transfer,* **102,** 236-241, (1980).

[29] **Gebhart, B.,** *Heat Transfer,* Mc-Graw Hill, NY, (1971).

انتقـال الحـرارة بالحمـل الحـر الانسيابي في حيـز مربع عند تسخـين جـزئي لجـدران عموديـة

عبدالحي محمد رضوان و جلال محمد زكي

كلية الهندسة ، قسم الهندسة الميكانيكية ، جامعة الملك عبد العزيز

جـــدة – المملكة العربية السعودية

المستخلص . أجريت دراسة عددية لانتقال الحرارة بالحمل الحر في حيز مربع معبأ بالهواء بوضع سخان جزئي ومباشر على جدار . إن الحيز كان في وضع عمودي وقد تم إبقاء جزء من جدار عمودي في درجة حرارة ثابتة بينما بقية الجدار وكذلك الجدار المقابل في درجة حرارة أقل . وقد عُزلت الجوانب العليا والسفلى من الحيز . وقد حُلّت المعادلات التفاضلية ذات البعدين الخاصة بحفظ المادة والطاقة وكمية الحركة باستخدام طريقة الفـروقـات المحـدودة لعـدة قـيم لرقم رالي تتـراوح بين $١٠^{٢}$–$١٠^{٦}$. ودُرست التغيرات في درجة الحرارة وحقول السريان مع زيادة رقم رالي وذلك لعدة مواضع للسخان . وقد وُجد من الدراسة أن المناطق الباردة المجاورة للسخان والتي تم إبقاؤها في درجة حرارة أقل تساعد على تكوين خلايا دوران ثانوية والتي تعتمد على رقم رالي وعلى موضع السخان . وبوجود التسخين الجزئي والمناطق الباردة على جدار واحد يتميز السريان بوجود طبقات متاخمة تحيط هذه المناطق بخلايا دوران منفصلة . وتتأثر التغيرات في رقم نوسلت المحلي بهذا النمط من السريان ويكون متوسط رقم نوسلت أكبر من ذلك عندما يكون شريط التسخين موضوعًا على جدار معزول . وقد وجد أن المكان الأمثل – في نطاق رقم رالي – هو منتصف الجدار $S/L = 0.5$. وهذه النتيجة دُعمت بنتائج تجارب سابقة .